

NEMO-3 DOUBLE BETA DECAY EXPERIMENT: LATEST RESULTS

A. S. BARABASH* (ON BEHALF OF THE NEMO COLLABORATION)

Institute of Theoretical and Experimental Physics, Moscow, 117218, Russia

**E-mail: barabash@itep.ru*

Latest results on $0\nu\beta\beta$, $0\nu\chi^0\beta\beta$ and $2\nu\beta\beta$ decays of different isotopes from NEMO-3 double beta decay experiment are presented. In particular, new limits at 90% C.L. on neutrinoless double beta decay of ^{100}Mo and ^{82}Se have been obtained, $T_{1/2} > 5.8 \times 10^{23}$ y and $T_{1/2} > 2.1 \times 10^{23}$ y, respectively.

Keywords: double beta decay; neutrino mass; particle tracking detectors.

1. Introduction

The experiments with solar, atmospheric, reactor and accelerator neutrinos have provided compelling evidences for the existence of neutrino oscillations driven by nonzero neutrino masses and neutrino mixing (see recent reviews ^{1,2,3} and reference therein). However, the experiments studying neutrino oscillations are not sensitive to the nature of the neutrino mass (Dirac or Majorana?) and provide no information on the absolute scale of the neutrino masses, since such experiments are sensitive only to the Δm^2 . The detection and study of $0\nu\beta\beta$ decay may clarify the following problems of neutrino physics (see discussions in Ref. ^{4,5}): (i) neutrino nature; is the neutrino a Dirac or a Majorana particle?, (ii) absolute neutrino mass scale (a measurement or a limit on m_1), (iii) the type of neutrino mass hierarchy (normal, inverted, or quasidegenerate), (iv) CP violation in the lepton sector (measurement of the Majorana CP-violating phases).

In connection with the $0\nu\beta\beta$ decay, the detection of double beta decay with the emission of two neutrinos ($2\nu\beta\beta$), which is allowed process of second order in the Standard Model, enables the experimental determination of nuclear matrix elements involved in the double beta decay processes. Accumulation of experimental information for the $2\nu\beta\beta$ processes (transitions to the ground

and excited states) promotes a better understanding of the nuclear part of double beta decay, and allows one to check theoretical schemes of nuclear matrix element (NME) calculations for the two neutrino mode as well as for the neutrinoless one.

The main objective of the NEMO-3 experiment is to seek the $0\nu\beta\beta$ decay of various isotopes (^{100}Mo , ^{82}Se , etc.) with a sensitivity to half-life up to $\sim n \times 10^{24}$ y. In addition, one of the tasks consists in studying, at a high level of precision, the $2\nu\beta\beta$ decay of a broad range of nuclei (^{100}Mo , ^{82}Se , ^{116}Cd , ^{150}Nd , ^{130}Te , ^{96}Zr and ^{48}Ca) and currently exploring all features of double beta decay processes.

The NEMO-3 experiment is a tracking experiment where, in contrast to experiments with ^{76}Ge ^{6,7}, one detect not only the total energy deposition but also the remaining parameters of the process, including the energy of individual electrons, their divergence angle, and the coordinate of an event in the source plane. Since June 2002, the NEMO-3 detector has operated at the Frejus Underground Laboratory (France) located at a depth of 4800 m w.e. Since February 2003, the detector has been routinely taking data.

2. The NEMO-3 detector

The detector has a cylindrical structure and consists of 20 identical sectors A thin (about

30-60 mg/cm²) source containing double beta-decaying nuclei and having a total area of 20 m² and a weight of up to 10 kg was placed in the detector. The energy of the electrons is measured by plastic scintillators (1940 individual counters), while the tracks are reconstructed on the basis of information obtained in the planes of Geiger cells (6180 cells) surrounding the source on both sides. The tracking volume of the detector is filled with a mixture consisting of $\sim 95\%$ He, 4% alcohol, 1% Ar and 0.1% water at slightly above atmospheric pressure. In addition, a magnetic field of strength of about 25 G that is parallel to the detector axis is created by a solenoid surrounding the detector. The magnetic field is used to identify electron-positron pairs to suppress this source of background.

The main characteristics of the detector are the following: the energy resolution of the scintillation counters lies in the interval 14-17% FWHM for electrons of energy 1 MeV; the time resolution is 250 ps for an electron energy of 1 MeV; and the accuracy in reconstructing of the vertex of $2e^-$ events is about 1 cm. The detector is surrounded by a passive shield consisting of 20 cm of steel and 30 cm of borated water. The level of radioactive impurities in structural materials of the detector and of the passive shield was tested in measurements with low-background HPGe detectors.

Measurements with the NEMO-3 detector revealed that tracking information, combined with time and energy measurements, makes it possible to suppress the background efficiently. That NEMO-3 can be used to investigate almost all isotopes of interest is a distinctive feature of this facility. At the present time, such investigations are being performed for seven isotopes; these are ¹⁰⁰Mo (6.9 kg), ⁸²Se (0.93 kg), ¹¹⁶Cd (0.4 kg), ¹⁵⁰Nd (36.6 g), ⁹⁶Zr (9.4 g), ¹³⁰Te (0.45 kg), and ⁴⁸Ca (7 g). In addition, foils from copper and

natural (not enriched) tellurium are placed in the detector for performing background measurements. A detailed description of the detector and its characteristics is presented in Ref. ⁸.

After starting the experiment, a small amount of radon was detected inside the tracking chamber. It was demonstrated that the major contribution was coming from laboratory air through small leaks. To solve the problem a tight tent surrounding the detector was built. The tent is fed with radon free air, coming from a radon trapping facility. The core of this facility is a charcoal tank operating at -50 °C. Radon is trapped inside the charcoal and decays while diffusing through it. So no regeneration is needed.

A reduction factor of 100 was achieved for the radon in the air inside the tent. The radon level in the tracking chamber dropped from 20-30 mBq/m³ to 4-5 mBq/m³. It is now the case that the remaining radon in the detector is dominated by the degassing of the construction components.

Thus there are two data sets. Phase I data corresponding to a higher radon background, and Phase II (since December 2004), with low background conditions.

3. Experimental results

3.1. ¹⁰⁰Mo results

A measurement of $2\nu\beta\beta$ decay was done with Phase I data, see Table 1 and Fig. 1(b) ⁹. Given the largest statistical data set in the world (219000 events) and a signal-to-background ratio (S/B) of 40, the single state dominance (SSD) mechanism ¹⁰ of the decay was confirmed. Also ¹⁰⁰Mo $2\nu\beta\beta$ decay to the excited 0^+ state (1130.29 keV) of ¹⁰⁰Ru was measured with a half life of $T_{1/2} = [5.7_{-0.9}^{+1.3}(\text{stat}) \pm 0.8(\text{syst})] \times 10^{20}$ years. All these results are important input for nuclear physics theory. They can be used to validate nuclear model for further $0\nu\beta\beta$ nuclear matrix elements calculations.

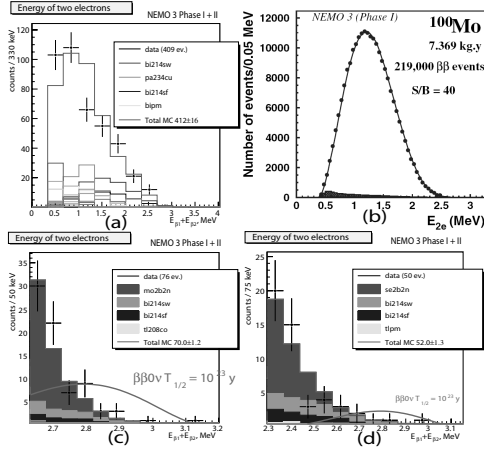


Fig. 1. (a) Background $\beta\beta$ spectrum in Cu foil (Phase I + II); (b) ^{100}Mo Phase I $2\nu\beta\beta$ spectrum; (c) ^{100}Mo (Phase I + Phase II) $2\nu\beta\beta$ spectrum at $Q_{\beta\beta}$; (d) ^{82}Se (Phase I + Phase II) $2\nu\beta\beta$ spectrum at $Q_{\beta\beta}$.

In the $0\nu\beta\beta$ decay search, no signal was found (Fig. 1(c)). The data for Phase I and Phase II were combined. A preliminary counting analysis shows 14 events in the window of interest [2.78–3.20] MeV, the expected background is 13.4 events, and $\beta\beta_{0\nu}$ efficiency is 8.4%. The effective time analyzed is 13 kg·y yielding a lower limit on the half-life of $T_{1/2} > 5.8 \times 10^{23}$ y (90% C.L.), corresponding to the effective neutrino mass $\langle m_\nu \rangle < 0.6 - 0.9$ eV using NME from Ref. ^{11,12,13} or $\langle m_\nu \rangle < 2.0 - 2.7$ eV using recent value of NME from Ref. ¹⁴.

In the hypothesis of a right-handed weak current, the limit is $T_{1/2} > 3.2 \times 10^{23}$ y (90% C.L.), corresponding to an upper limit of the coupling constant of $\lambda < 1.8 \times 10^{-6}$ using NME from Ref. ¹⁵.

3.2. ^{82}Se results

2570 $2\nu\beta\beta$ events were registered during Phase I of the experiment, with a S/B ratio equal to about 4, and a half-life given in Table 1.

After the preliminary analysis of 1.76 kg·y of Phase I and Phase II data, see Fig.

1(d), 7 events were found in the window [2.62–3.20] MeV, with the expected background 6.4 events, $0\nu\beta\beta$ efficiency of 14.4% yielding a lower limit on the half-life of $T_{1/2} > 2.1 \times 10^{23}$ y (90% C.L.), which corresponds to an upper mass limit of $\langle m_\nu \rangle < 1.2 - 2.5$ eV using NME from Ref. ^{11,12,13} or $\langle m_\nu \rangle < 2.3 - 3.2$ eV using recent value of NME from Ref. ¹⁴.

In the hypothesis of a right-handed weak current, the limit is $T_{1/2} > 1.2 \times 10^{23}$ y (90% C.L.), corresponding to an upper limit of the coupling constant of $\lambda < 2.8 \times 10^{-6}$ using NME from Ref. ¹⁶.

3.3. $2\nu\beta\beta$ decay of other nuclei

Phase I data for four other isotopes (^{116}Cd , ^{150}Nd , ^{96}Zr and ^{48}Ca) were analyzed and their half-lives measured, see Table 1 with preliminary results. This should be a very important guide for nuclear theory. Since all isotopes are measured with the same device and at the same time, the half-life ratio has a very small systematic uncertainty, while statistical errors will reach a few per cent.

3.4. Neutrinoless double beta decay with Majoron emission

8023 h of Phase I data were analyzed. The half-life limits for ^{100}Mo and ^{82}Se for the different modes with different value of spectral index n are presented in Table 2 (see details in Ref. ¹⁷). In particular, limits on "ordinary" Majoron with $n = 1$ are $T_{1/2} > 2.7 \times 10^{22}$ y (90% C.L.) for ^{100}Mo and $T_{1/2} > 1.5 \times 10^{22}$ y (90% C.L.) for ^{82}Se . Using NME from Ref. ^{11,12,13} one can obtain limits on coupling constant of Majoron to neutrino $\langle g_{ee} \rangle < (0.4 - 0.7) \times 10^{-4}$ and $< (0.7 - 1.4) \times 10^{-4}$ respectively. If one uses NME from Ref. ¹⁴ then limits are $< (1.3 - 1.8) \times 10^{-4}$ for ^{100}Mo and $< (1.3 - 1.8) \times 10^{-4}$ for ^{82}Se .

Table 1. Main results on $2\nu\beta\beta$ decays.

Nuclei	Measurement time, days	Number of 2ν events	$T_{1/2}$, y
^{100}Mo	389	219000	$[7.11 \pm 0.02(\text{stat}) \pm 0.54(\text{syst})] \times 10^{18}$
$^{100}\text{Mo}-^{100}\text{Ru}(0_1^+)$	334.3	38	$[5.7_{-0.9}^{+1.3}(\text{stat}) \pm 0.8(\text{syst})] \times 10^{20}$
^{82}Se	389	2750	$[9.6 \pm 0.3(\text{stat}) \pm 1.0(\text{syst})] \times 10^{19}$
^{116}Cd	168.4	1371	$[2.8 \pm 0.1(\text{stat}) \pm 0.3(\text{syst})] \times 10^{19}$
^{150}Nd	168.4	449	$[9.7 \pm 0.7(\text{stat}) \pm 1.0(\text{syst})] \times 10^{18}$
^{96}Zr	168.4	72	$[2.0 \pm 0.3(\text{stat}) \pm 0.2(\text{syst})] \times 10^{19}$
^{48}Ca	446.7	51	$[3.9 \pm 0.7(\text{stat}) \pm 0.6(\text{syst})] \times 10^{19}$

Table 2. Limits (in years) on $0\nu\beta\beta$ decay with Majoron emission for ^{100}Mo and ^{82}Se . n - spectral index.

Nuclei	n = 1	n = 2	n = 3	n = 7
^{100}Mo	$> 2.7 \times 10^{22}$	$> 1.7 \times 10^{22}$	$> 1.0 \times 10^{22}$	$> 7.0 \times 10^{19}$
^{82}Se	$> 1.5 \times 10^{22}$	$> 6 \times 10^{21}$	$> 3.1 \times 10^{21}$	$> 5.0 \times 10^{20}$

4. Conclusion

The NEMO-3 detector has been running reliably since February 2003 and since December 2004 under "low Rn" background conditions. The $2\nu\beta\beta$ decay has been measured for ^{48}Ca , ^{82}Se , ^{96}Zr , ^{100}Mo , ^{116}Cd , and ^{150}Nd . In addition $2\nu\beta\beta$ decay of ^{100}Mo to the 0^+ (1130.29 keV) excited state of ^{100}Ru has been investigated. No evidence for $0\nu\beta\beta$ is found.

At present, NEMO Collaboration continue data analysis and new results will be obtained soon. The NEMO-3 detector is continuing to collect data and for 5 y of measurements the sensitivity of experiment for $0\nu\beta\beta$ decay will be increased up to $\sim 2 \times 10^{24}$ y for ^{100}Mo and $\sim 8 \times 10^{23}$ y for ^{82}Se .

Acknowledgments

A portion of this work was supported by grant from INTAS (03051-3431).

References

1. J.W.F. Valle, hep-ph/0608101.
2. S.M. Bilenky, hep-ph/0607317.
3. R.N. Mohapatra and A.Y. Smirnov, hep-ph/0603118.
4. S. Pascoli, S.T. Petcov and W. Rodejohann, *Phys. Lett.* **B558**, 141 (2003).
5. S. Pascoli, S.T. Petcov and T. Schwetz, *Nucl. Phys.* **B734**, 24 (2006).
6. H.V. Klapdor-Kleingrothaus *et al.*, *Eur. Phys. J.* **A12**, 147 (2001).
7. C.E. Aalseth *et al.*, *Phys. Rev.* **C65**, 09007 (2002).
8. R. Arnold *et al.*, *Nucl. Instr. Meth.* **A536**, 79 (2005).
9. R. Arnold *et al.*, *Phys. Rev. Lett.* **95**, 182302 (2005).
10. F. Simkovic *et al.*, *J. Phys.* **G27**, 2233 (2001).
11. F. Simkovic *et al.*, *Phys. Rev.* **C60**, 055502 (1999).
12. S. Stoica and H.V. Klapdor-Kleingrothaus *et al.*, *Nucl. Phys.* **A694**, 269 (2001).
13. O. Civitarese and J. Suhonen, *Nucl. Phys.* **A729**, 867 (2003).
14. V. Rodin *et al.*, *Nucl. Phys.* **A766**, 107 (2006).
15. J. Suhonen, *Nucl. Phys.* **A700**, 649 (2002).
16. M. Aunola and J. Suhonen, *Nucl. Phys.* **A643**, 207 (1998).
17. R. Arnold *et al.*, *Nucl. Phys.* **A765**, 483 (2006).